Binuclear Complexes as Building Blocks for Polynuclear Complexes with High-Spin Ground States: Synthesis and Structure of a Tetranuclear Nickel Complex with an $S = 4$ Ground State

Berthold Kersting,*[a] Gunther Steinfeld,[a] and Dieter Siebert[b]

Abstract: The coordinatively unsaturated dinickel(II) complex $[(L^2)Ni_2](BPh_4)_2$ (**2**), where $(L^2)^{2-}$ represents the dianionic form of the 'N_4S_2' ligand *N*,*N*′-bis(2-thio-3-aminomethyl-5-*tert*-butylbenzyl)-propane-1,3-diamine), has been investigated with respect to its ability to function as a building block for the preparation of polynuclear nickel complexes with a high-spin ground state. Treatment of **2** with pyridazine (pydz) followed by addition of two equivalents of NH_4SCN afforded the dinuclear μ-pyridazine complex $[(L^2)Ni_2(\mu\text{-pydz})(NCS)_2]$ (**4**). The reaction of **2** with pyridazine and NaN_3 in a 1:1:1 molar ratio gave the tetranuclear nickel(II) complex $[\{(L^2)Ni_2(\mu\text{-pydz})(N_3)\}_2](BPh_4)_2$ (**5**). Both complexes have been characterized by X-ray crystallography and variable-temperature magnetic susceptibility studies. In complex **4** two *fac*-$(SCN)N_2Ni^{II}$ units are linked by two thiophenolate sulfur atoms and a μ-pydz ligand to give a $(SCN)N_2Ni(\mu\text{-S})_2(\mu\text{-pydz})NiN_2(NCS)$ core structure with a pseudoconfacial bioctahedral geometry. The two NCS^- groups occupy opposite coordination sites, each is in a *cis* position to the pydz bridge. Analyses of the susceptibility data indicate the presence of an intramolecular ferromagnetic exchange interaction between the two Ni^{II} ($S = 1$) ions. Complex **5** is composed of two binuclear $[(L^2)Ni_2(\mu\text{-pydz})]^{2+}$ subunits which are linked by two azide ions to give a rectangular array of four six-coordinate Ni^{II} ions. The binuclear $[(L^2)Ni_2(\mu\text{-pydz})]^{2+}$ fragments in **4** and **5** are isostructural. Analyses of the susceptibility data of **5** reveal ferromagnetic exchange interactions between the Ni^{II} ions of the binuclear subunit as well as for the $\mu_{1,3}$-N_3-bridged Ni^{II} ions. Thus, compound **4** has an $S = 2$ ground state, whereas in **5** it is $S = 4$.

Keywords: magnetic properties · nickel · N,S ligands · polynuclear complexes

Introduction

The synthesis of polynuclear transition metal complexes with a large number of unpaired electrons in their spin ground state is currently attracting much interest, because such compounds often display unusual magnetic properties.[1] The self-organization of first-row transition metal ions and suitable bridging ligands has proved to be a very powerful strategy for the well-defined arrangement of metal ions;[2, 3] however, the type of magnetic exchange interaction between the metal ions is difficult to predict. An alternative approach would be the replacement of single metal ions by discrete binuclear complexes with a predefined pair state and free coordination sites for crosslinking by suitable bridging ligands.

We have recently reported on binuclear nickel complexes of the amine – thiophenolate ligands H_1L and H_2L^2.[4, 5] While the tridentate ligand forms a confacial bioctahedral complex **1** in which two paramagnetic N_3Ni^{II} units are linked by three thiophenolate sulfur functions, the hexadentate ligand H_2L^2 generates a 1:1 complex **2** with two planar NiN_2S_2 coordination units. As the latter compound is a coordinatively unsaturated species, we have investigated the possibility of generating a Ni^{II}_4 complex by linking two such units through additional bridging ligands in the hope of obtaining a paramagnetic complex. We report here on our findings.

Results and Discussion

Preparation and structure of complexes: We have previously shown that reactions of **2** with monodentate coligands L′ (NCS^-, N_3^-) yield purple neutral complexes of the type $[(L^2)Ni_2(L')_2]$ with adjacent four-coordinate NiN_2S_2 and six-coordinate $NiN_2S_2L'_2$ sites, not bioctahedral complexes.[5] We

[a] Dr. B. Kersting, Dipl.-Chem. G. Steinfeld
Institut für Anorganische und Analytische Chemie
Universität Freiburg
Albertstrasse 21, 79104 Freiburg (Germany)
Fax: (+49) 761-203-5987
E-mail: kerstber@sun2.ruf.uni-freiburg.de

[b] Prof. Dr. D. Siebert
Institut für Physikalische Chemie, Universität Freiburg
Albertstrasse 23a, 79104 Freiburg (Germany)

Supporting information for this article is available on the WWW under http://www.wiley-vch.de/home/chemistry or from the author.

  0947-6539/01/0719-4253 $ 17.50+.50/0

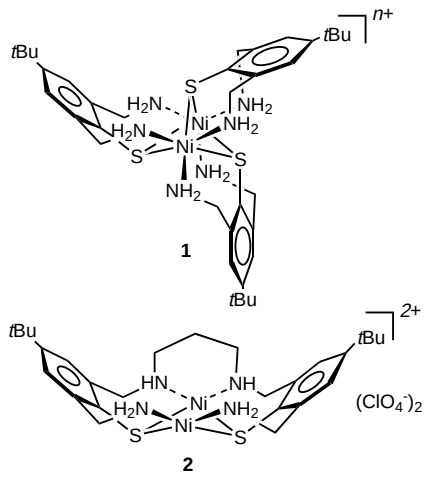

have now found that such complexes form when pyridazine (pydz) is added prior to the addition of the coligand L′. Thus, treatment of **2** with one equivalent of pydz followed by addition of two equivalents of NH_4SCN affords a brown solution from which a product of composition $[(L^2)Ni_2(\mu\text{-pydz})(NCS)_2]$ (**4**) precipitates in high yield (Scheme 1). The dicationic μ-pyridazine complex $[(L^2)Ni_2(\mu\text{-pydz})(L')_2]^{2+}$ (**3**) with two labile solvent molecules ($L' = CH_3CN$) can be formulated as an intermediate.

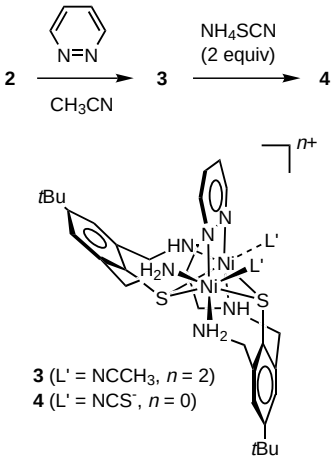

Scheme 1. Preparation of complex **4**.

The molecular structure of **4** was characterized by X-ray crystal structure analysis. Figure 1 shows a neutral molecule $[(L^2)Ni_2(\mu\text{-pydz})(NCS)_2]$ in crystals of **4**. Selected bond lengths and angles are summarized in Table 1. The Ni atoms are triply bridged by two S atoms from the amine-thiolate ligand and a pydz moiety which leads to a Ni···Ni distance of 3.340(1) Å. The N-bound thiocyanate groups are found in terminal positions on opposite sides of the molecule. Both are in a *cis* position relative to the pydz ligand. The amine nitrogen atoms of $(L^2)^{2-}$ complete the pseudooctahedral NiN_4S_2 coordination units. Notably, the corresponding bond lengths at Ni(1) and Ni(2) differ only slightly. With respect to the cryomagnetic properties described below, it is also of importance to note that there are no intermolecular hydrogen

Table 1. Selected bond lengths [Å] and angles [°] for **4**.

Ni(1)–S(1)	2.440(1)	Ni(2)–S(1)	2.469(1)
Ni(1)–S(2)	2.475(1)	Ni(2)–S(2)	2.466(1)
Ni(1)–N(1)	2.116(3)	Ni(2)–N(2)	2.084(3)
Ni(1)–N(3)	2.140(3)	Ni(2)–N(4)	2.119(3)
Ni(1)–N(5)	2.114(3)	Ni(2)–N(6)	2.114(3)
Ni(1)–N(7)	2.073(4)	Ni(2)–N(8)	2.077(4)
Ni(1)···Ni(2)	3.340(1)		
S(1)-Ni(1)-S(2)	82.02(5)	S(1)-Ni(2)-S(2)	81.63(5)
N(1)-Ni(1)-S(1)	94.22(10)	N(2)-Ni(2)-S(1)	90.71(10)
N(1)-Ni(1)-S(2)	93.17(10)	N(2)-Ni(2)-S(2)	96.18(11)
N(1)-Ni(1)-N(3)	92.05(13)	N(2)-Ni(2)-N(4)	88.96(14)
N(1)-Ni(1)-N(5)	175.97(14)	N(2)-Ni(2)-N(6)	175.13(14)
N(1)-Ni(1)-N(7)	87.59(14)	N(2)-Ni(2)-N(8)	86.89(14)
N(3)-Ni(1)-S(1)	171.95(10)	N(4)-Ni(2)-S(1)	173.98(10)
N(3)-Ni(1)-S(2)	92.61(10)	N(4)-Ni(2)-S(2)	92.43(10)
N(3)-Ni(1)-N(5)	88.62(13)	N(4)-Ni(2)-N(6)	92.23(14)
N(3)-Ni(1)-N(7)	92.03(14)	N(4)-Ni(2)-N(8)	87.95(14)
N(5)-Ni(1)-S(1)	85.48(10)	N(6)-Ni(2)-S(1)	88.60(10)
N(5)-Ni(1)-S(2)	90.78(10)	N(6)-Ni(2)-S(2)	88.49(10)
N(5)-Ni(1)-N(7)	88.41(14)	N(6)-Ni(2)-N(8)	88.44(14)
N(7)-Ni(1)-S(1)	93.27(11)	N(8)-Ni(2)-S(1)	98.03(11)
N(7)-Ni(1)-S(2)	175.27(11)	N(8)-Ni(2)-S(2)	176.92(11)
Ni(1)-S(1)-Ni(2)	85.76(5)	Ni(1)-S(2)-Ni(1)	85.05(5)

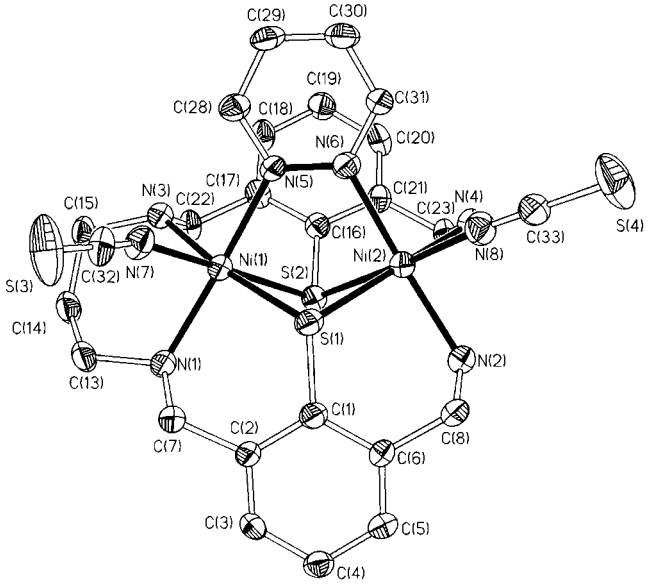

Figure 1. Molecular structure of the neutral complex $[(L^2)Ni_2(\mu\text{-pydz})(NCS)_2]$ in crystals of **4**. Thermal ellipsoids are drawn at the 50% probability level. *tert*-Butyl groups and hydrogen atoms are omitted for clarity.

bonding interactions between the complexes. Therefore, despite a relatively short intermolecular Ni···Ni distance of 7.287(1) Å, there is no possibility for a superexchange pathway between the complexes.

To test whether **2** can be used as a building block for polynuclear complexes, the NCS^- ligand in the above reaction was replaced by NaN_3 (Scheme 2). The azide ion is known for its tendency to form bridges between metal atoms.[6] A brown solid of composition $[\{(L^2)Ni_2(\mu\text{-pydz})(\mu_{1,3}\text{-}N_3)\}_2](BPh_4)_2$ (**5**) was obtained in 74% yield. The characteristic $\nu(N_3^-)$ absorption band at 2065 cm^{-1} in the IR spectrum of **5** was the first sign of the coordination of the azide ion. The X-ray crystal structure of **5** then complemented the infrared work and

0947-6539/01/0719-4254 $ 17.50+.50/0 *Chem. Eur. J.* **2001**, *7*, No. 19

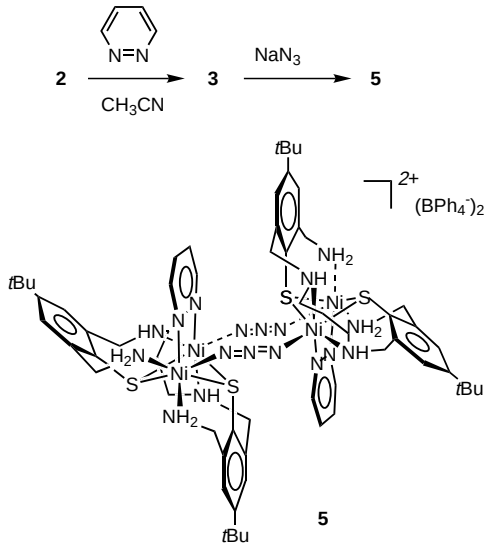

Scheme 2. Preparation of complex **5**.

showed the successful formation of a tetranuclear Ni^{II} complex (Figure 2). Two $[(L^2)Ni_2(\mu\text{-pydz})]^{2+}$ units are linked through two $\mu_{1,3}$-N_3^- ions to give a rectangular array of four six-coordinate Ni^{II} ions. In the solid state the dication possesses local C_i symmetry. The Ni···Ni distance of the

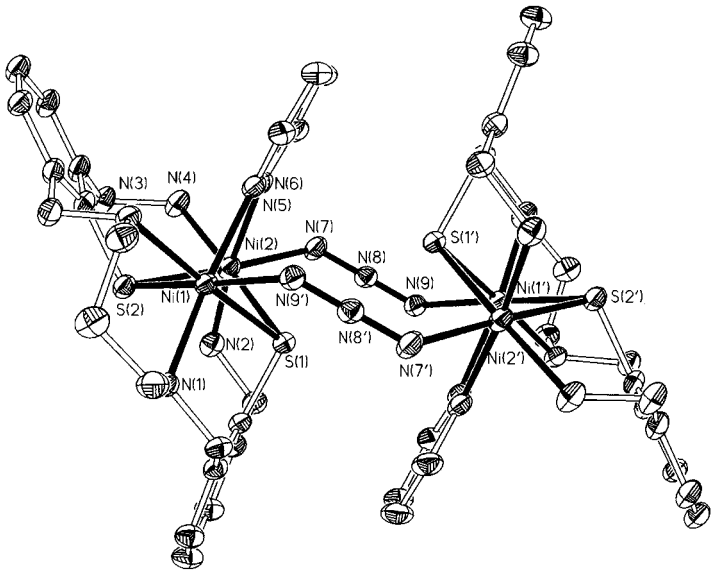

Figure 2. Molecular structure of the cation $[\{(L^2)Ni_2(\mu\text{-pydz})(N_3)\}_2]^{2+}$ in crystals of **5**. Thermal ellipsoids are drawn at the 50% probability level. *tert*-Butyl groups and hydrogen atoms are omitted for clarity. Symmetry code used to generate equivalent atoms: $1-x, 1-y, -z$ (′).

binuclear subunit at 3.283(1) Å is only slightly shorther than in **4** (Table 2). The separation of the $\mu_{1,3}$-N_3-bridged nickel atoms is significantly longer, at 5.322(1) Å. The tetranuclear units are well separated from each other by the sterically demanding tetraphenylborate anions. The shortest intermolecular Ni···Ni distance at 11.116(1) Å is even longer than in **4**. These results clearly show that the dinuclear nickel(II) complex **2** can be used as a building block for the preparation of a higher nuclearity species.

Table 2. Selected bond lengths [Å] and angles [°] for **5**.[a]

Ni(1)–S(1)	2.4354(11)	Ni(2)–S(1)	2.4159(12)
Ni(1)–S(2)	2.4283(13)	Ni(2)–S(2)	2.4198(12)
Ni(1)–N(1)	2.112(3)	Ni(2)–N(2)	2.087(4)
Ni(1)–N(3)	2.131(3)	Ni(2)–N(4)	2.128(3)
Ni(1)–N(5)	2.134(3)	Ni(2)–N(6)	2.107(4)
Ni(1)–N(9′)	2.142(3)	Ni(2)–N(7)	2.156(3)
Ni(1)···Ni(2)	3.283(1)	N(7)–N(8)	1.181(4)
Ni(1)···Ni(2′)	5.322(1)	N(8)–N(9)	1.163(4)
Ni(1)···Ni(1′)	6.332(1)		
S(1)-Ni(1)-S(2)	81.92(4)	S(1)-Ni(2)-S(2)	82.49(3)
N(1)-Ni(1)-S(1)	94.13(8)	N(2)-Ni(2)-S(1)	92.93(10)
N(1)-Ni(1)-S(2)	96.15(9)	N(2)-Ni(2)-S(2)	96.43(10)
N(1)-Ni(1)-N(3)	91.68(12)	N(2)-Ni(2)-N(4)	90.23(14)
N(1)-Ni(1)-N(5)	172.75(13)	N(2)-Ni(2)-N(6)	172.26(13)
N(1)-Ni(1)-N(9′)	87.94(13)	N(2)-Ni(2)-N(7)	85.61(14)
N(3)-Ni(1)-S(1)	172.63(9)	N(4)-Ni(2)-S(1)	174.17(9)
N(3)-Ni(1)-S(2)	92.96(9)	N(4)-Ni(2)-S(2)	92.29(9)
N(3)-Ni(1)-N(5)	88.34(12)	N(4)-Ni(2)-N(6)	90.19(14)
N(3)-Ni(1)-N(9′)	90.21(12)	N(4)-Ni(2)-N(7)	86.55(13)
N(5)-Ni(1)-N(9′)	84.82(13)	N(6)-Ni(2)-S(1)	87.34(9)
N(5)-Ni(1)-S(2)	91.08(10)	N(6)-Ni(2)-S(2)	91.27(9)
N(5)-Ni(1)-S(1)	86.47(9)	N(6)-Ni(2)-N(7)	86.70(13)
N(9′)-Ni(1)-S(1)	94.52(9)	N(7)-Ni(2)-S(1)	98.57(9)
N(9′)-Ni(1)-S(2)	174.74(9)	N(7)-Ni(2)-S(2)	177.66(10)
Ni(1)-S(1)-Ni(2)	85.18(4)	Ni(1)-S(2)-Ni(2)	85.25(4)
N(8)-N(7)-Ni(2)	123.8(3)	N(8′)-N(9′)-Ni(1)	126.8(3)

[a] Symmetry code used to generate equivalent atoms: $1-x, 1-y, -z$ (′).

Magnetic susceptibility: To gain insight into the electronic structures of **4** and **5** variable-temperature magnetic susceptibility data were measured between 2.0 and 290 K by using a SQUID magnetometer. Figure 3 shows the experimental data in the form of $\chi_M T$ versus T plots.

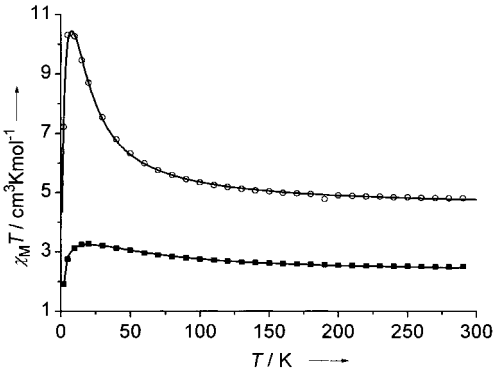

Figure 3. Plots of $\chi_M T$ against T for **4** and **5**. Experimental data are shown as solid squares (for **4**) or as open circles (for **5**). The full lines represent the best theoretical fits.

For complex **4** the product $\chi_M T$ gradually increases from 2.50 $cm^3 Kmol^{-1}$ at 295 K (4.47 μ_B per dinuclear complex) to a maximum of 3.27 $cm^3 Kmol^{-1}$ (5.12 μ_B) at 20 K,[7] and then decreases rapidly to 1.92 $cm^3 Kmol^{-1}$ at 2 K. This behavior is typical for an intramolecular ferromagnetic exchange interaction between the two Ni^{II} ions ($S_1 = S_2 = 1$) leading to an $S = 2$ ground state of **4**.[8] The cryomagnetic behavior of complex **5** is similar but not identical to that of **4**. With decreasing temperature, the value of the product $\chi_M T$ increases more and more rapidly, from 4.80 $cm^3 Kmol^{-1}$ at

290 K (6.20 μ_B per tetranuclear complex) to 10.03 $cm^3 Kmol^{-1}$ (9.08 μ_B) at 5 K. On lowering the temperature further the observed values decrease rapidly to a minimum value of 7.21 $cm^3 Kmol^{-1}$ at 2 K. The effective magnetic moment at 5 K is comparable with the spin-only value of 8.94 μ_B for $S_T = 4$ resulting from the ferromagnetic coupling of four Ni^{II} ions ($S = 1$, $g = 2.11$).[9] From a formal point of view, the $S_T = 4$ ground state of **5** results from an addition (not substraction) of the pair states of the two constituent $[(L^2)Ni_2(\mu\text{-pydz})]^{2+}$ subunits.

To model the experimental data a specific spin Hamiltonian was developed for each compound with a coupling scheme based on the molecular structure observed in the solid state. The resulting Hamiltonian matrix was diagonalized numerically to obtain the energies of the spin states, which on substitution into the van Vleck formula give the theoretical values for the magnetic susceptibility. A least-squares program then compared calculated and observed susceptibility curves and changed the parameters to get the best fit.

Thus, the magnetic susceptibility data for compound **4** were analyzed by using the isotropic Heisenberg-Dirac-van-Vleck (HDvV) exchange Hamiltonian [Eq. (1)] for dinuclear com-

$$\hat{H} = -2J\hat{S}_1\hat{S}_2 + \sum_{i=1}^{2}\left(D\hat{S}_{iz}^2 + g_i\mu_B B\hat{S}_{iz}\right) \quad (1)$$

plexes ($S_1 = S_2 = 1$), which includes two additional terms to account for Zeeman splitting and single-ion zero field interactions (DS_z^2). To reduce the number of variables the D and g values were considered to be identical for all positions. As can be seen from Figure 3 the HDvV model produces a good fit to the data with the parameters $J = +11.5\ cm^{-1}$, $g = 2.15$, and $|D| = 1.4\ cm^{-1}$. Notably, inclusion of the zero-field splitting parameter improved the low-temperature fit significantly but it by no means represents an accurate value.

The magnetic susceptibility data for compound **5** were analyzed by using the Hamiltonian in Equation (2).

$$\hat{H} = -2J_1(\hat{S}_1\hat{S}_2 + \hat{S}_3\hat{S}_4) - 2J_2(\hat{S}_2\hat{S}_3 + \hat{S}_1\hat{S}_4) + \sum_{i=1}^{4}(D\hat{S}_{iz}^2 + g_i\mu_B B\hat{S}_{iz}) \quad (2)$$

In this model J_1 ($= J_{12} = J_{34}$) represents the exchange interaction between the nickel ions in the binuclear subunit, whereas J_2 describes the interaction between the azido-bridged nickel centers. The D and g values were again considered to be identical. Note that the assignment of J_1 to the interaction between S_1 and S_2 is arbitrary. It could as well be between S_1 and S_4.[10] The best fit to the data yielded two *ferromagnetic* coupling constants $J_1 = +6.47\ cm^{-1}$ and $J_2 = +3.59\ cm^{-1}$, a g value of 2.11 and a zero-field splitting parameter $D = -0.068\ cm^{-1}$ (Figure 3). When the zero-field splitting is neglected ($D = 0$ fixed), the fit yields $J_1 = +6.01\ cm^{-1}$, $J_2 = +3.81\ cm^{-1}$, and $g = 2.11$. With the latter values one can calculate that the first excited state, a spin septet, is separated by $+15.2\ cm^{-1}$ from the $S_T = 4$ spin ground state.

The presence of a ferromagnetic exchange interaction in **4** can be understood in terms of the Goodenough – Kanamori rules for superexchange.[11] For the following discussion we assume that the dominant pathway for magnetic exchange is propagated through the thiolate sulfur atoms, although a significant contribution from the bridging pyridazine unit cannot be ruled out. For face-sharing bioctahedral nickel complexes a ferromagnetic interaction is predicted in the case that the Ni-X-Ni bridging angle is at 90°. If the bridging angle is smaller than 90° the orthogonality of the magnetic orbitals is cancelled and antiferromagnetic pathways become available to produce a change of the sign of J. An antiferromagnetic exchange interaction, for example, is found in tris(chloro)- or tris(thiophenolato)-bridged complexes, where the average Ni-X-Ni bond angle is found in the range 78° to 80°.[12] In tris(phenolato)-bridged species, on the other hand, the Ni-O-Ni angles are wider at 90 ± 8°, and therefore the spins align parallel.[13, 14] For **4** the average Ni-S-Ni bond angle is 85.40(5)°, which is more obtuse than in tris(thiophenolate)-bridged complexes, and in the range where the ferromagnetic pathway is the preferred one.

We now attempt to qualitatively rationalize the experimentally determined $S_T = 4$ ground state of **5**. According to the arguments detailed above for **4** the coupling between the nickel(II) ions in the binuclear subunit should be ferromagnetic in nature, because the average Ni-S-Ni angle at 85.22(4)° is nearly identical to that in **4**. This is indeed the case, however, the magnitude of the interaction is smaller than in **4**, irrespective of the assignment to J_1 or J_2. It could be due to the different coordination environments of the metal ions in the two complexes. The ferromagnetic coupling between the nickel centers in the Ni^{II}-($\mu_{1,3}$-N_3)-Ni^{II} fragment is also rather atypical. In general, all binuclear Ni compounds with this motif are known to exhibit antiferromagnetic interactions. Recently, Escuer et al. have shown that the magnitude of the antiferromagnetic exchange coupling constant depends on the Ni-N-N bond angle as well as on the Ni-N-N-N-Ni torsional angle. If the former angle exceeds 155° and (or) the latter 55° the exchange interactions become ferromagnetic.[15, 16] Our observation of a weak ferromagnetic coupling in **5** showing a large Ni-N-N-N-Ni torsional angle of 76.4° is in good agreement with the reported trend.

Conclusion

The synthesis of a novel tetranuclear nickel complex with an $S_T = 4$ ground state has been described. Our route differs from previous examples in that a discrete binuclear dinickel(II) complex with a predefined $S = 2$ pair state has been used as a building block.[17] We are currently probing the possibility of whether the pyridazine unit in **5** can be substituted by a 1,2,4,5-tetrazine unit to access an octanuclear nickel(II) complex with an $S_T = 8$ spin ground state.

Experimental Section

The synthesis of the perchlorate salt of **2**, $[(L^2)Ni_2](ClO_4)_2$, has been described previously.[5] The synthesis of the tetraphenylborate salt is described below.

0947-6539/01/0719-4256 $ 17.50+.50/0 *Chem. Eur. J.* **2001**, *7*, No. 19

$[(L^2)Ni_2](BPh_4)_2$ (2): A solution of $NaBPh_4$ (1.37 g, 4.00 mmol) in methanol (10 mL) was added at 60 °C to a solution of $[(L^2)Ni_2](ClO_4)_2$ (0.40 g, 0.50 mmol) in methanol (60 mL). After stirring for 30 min, the suspension was cooled in an ice-bath. The red solid was isolated by filtration, washed with cold methanol, and dried in air. The yield was 534 mg (86 %). M.p. 244–246 °C. IR (KBr disk): $\tilde{\nu}$ = 3250, 3190 (NH, NH_2), 735, 707 cm^{-1} (BPh_4^-); ^1H NMR (300 MHz, [D$_2$]dichloromethane, 25 °C, TMS): δ = 7.41–6.89 (m, 44H; ArH), 3.25 (d, ^3J = 12.7 Hz, 2H; ArCH*H*NH_2), 3.00 (d, ^3J = 12.2 Hz, 2H; ArCH*H*NH), 2.70 (d, ^3J = 11.8 Hz, 2H; ArC*H*HNH), 2.65 (t, ^3J = 12.2 Hz, 2H; ArC*H*HNH_2), 2.35 (q, 2H; $NHCH_2$), 1.80 (d, 2H; CH_2), 1.65 (d, 2H; CH_2), 1.40 (m, 2H; NH), 1.28 (s, 18H; CH_3), 0.92 (m, 2H; CH_2), 0.42 (d, 2H; NH*H*), 0.10 (m, 2H; N*H*H); UV/Vis (CH_2Cl_2): λ_{max} (ε) = 318 (2575), 378 (3484), 497 nm (780 $mol^{-1}dm^3cm^{-1}$); elemental analysis calcd (%) for $C_{75}H_{82}B_2N_4Ni_2S_2$ (1242.62): C 72.49, H 6.65, N 4.51; found: C 72.23, H 6.72, N 4.22.

$[(L^2)Ni_2(\mu\text{-pydz})(NCS)_2]$ (4): A solution of pyridazine (8.8 mg, 0.11 mmol) in acetonitrile (3 mL) was added to a solution of **2** (124 mg, 0.100 mmol) in a mixture of methanol (12 mL) and acetonitrile (12 mL). The color of the solution changed immediately from red to brown. After the reaction mixture was stirred for further 1 h a solution of NH_4SCN (16.7 mg, 0.220 mmol) in methanol (1 mL) was added. Upon standing in an open vessel at ambient temperature for 2–3 days brown-green, needle-shaped crystals of **4** precipitated. Yield: 69 mg (72 %). M.p. 234–237 °C (decomp); IR(KBr disk): $\tilde{\nu}$ = 2089 cm^{-1} (CN); UV/Vis (DMF): $\lambda_{max}(\varepsilon)$ = 596(80), 1012 nm (43 $mol^{-1}dm^3m^{-1}$); elemental analysis (%) calcd for $C_{33}H_{46}N_8Ni_2S_4$ (800.42) C 49.52, H 5.79, N 14.00; found: C 49.17, H 5.62, N 13.78.

$[\{(L^2)Ni_2(\mu\text{-pydz})(\mu_{1,3}\text{-}N_3)\}_2](BPh_4)_2$ (5): A solution of pyridazine (8.8 mg, 0.11 mmol) in acetonitrile was added to a solution of **2** (124 mg, 0.100 mmol) in acetonitrile. After 1 h, a solution of NaN_3 (6.5 mg, 0.10 mmol) in methanol (1 mL) was added and the reaction mixture was heated at 60 °C for 10 min. The solution was filtered while hot and left to stand in an open vessel. Brown plates precipitated within two days. Yield: 77 mg (74 %). M.p. 264–266 °C (decomp); IR(KBr disk): $\tilde{\nu}$ = 2065 cm^{-1} (N_3^-); UV/Vis (DMF): λ_{max} (ε) = 615 (87), 1021 nm (46 $mol^{-1}dm^3m^{-1}$); elemental analysis (%) calcd for $C_{110}H_{132}B_2N_{18}Ni_4S_4$ (2091.01): C 63.19, H 6.36, N 12.06; found: C 62.97, H 6.20, N 11.78.

Physical measurements: Melting points were determined in capillaries and are uncorrected. ^1H NMR spectra were recorded on a Varian 300 unity spectrometer. IR spectra were taken on a Bruker VECTOR 22 FT-IR spectrophotometer as KBr pellets. Electronic absorption spectra were recorded on a Jasco V-570 UV/Vis/near IR spectrophotometer. EPR spectra were recorded by a conventional Varian X-band spectrometer with 100 kHz modulation. Temperature-dependent magnetic susceptibility measurements on powdered solid samples were carried out on a SQUID magnetometer (MPMS Quantum Design) over the temperature range 2.0–293 K. The magnetic field applied was 1.00 Tesla. The observed susceptibility data were corrected for underlying diamagnetism by using Pascal's constants.

Crystal structure determinations: Single crystals of $\mathbf{4}\cdot MeCN\cdot H_2O$ and of $\mathbf{5}\cdot 2MeCN\cdot MeOH$ suitable for X-ray structure analysis were obtained by slow evaporation of acetonitrile/methanol solutions of the complexes. The crystals were mounted on glass fibers using perfluoropolyether oil. Intensity data were collected at 180(2) K, using a Bruker SMART CCD diffractometer. Graphite-monochromated $Mo_{K\alpha}$ radiation (λ = 0.71073 Å) was used throughout. The data were processed with SAINT[18] and corrected for absorption using SADABS[19] (transmission factors: 0.76–1.00 for **4**, 0.78–1.00 for **5**).

Crystal data for $\mathbf{4}\cdot MeCN\cdot H_2O$: $C_{35}H_{51}N_9Ni_2OS_4$ (M_r = 859.51); crystal size 0.50 × 0.38 × 0.33 mm^3; triclinic, space group $P\bar{1}$ (no. 2), with a = 11.212(2), b = 13.674(3), c = 14.747(3) Å, α = 94.42(3), β = 96.99(3), γ = 111.35(3)°, Z = 2, V = 2072(1) Å^3, ρ_{calcd} = 1.378 g cm^{-3}, $2\theta_{max}$ = 56.66°, $\mu(Mo_{K\alpha})$ = 1.150 mm^{-1}, 19064 reflections measured, 9748 unique (R_{int} = 0.0534), 4593 observed reflections [$I > 2\sigma(I)$]. The structure was solved by direct methods using the program SHELXS-86;[20] and refined by full-matrix least-squares techniques against F^2 using SHELXL-93.[21] All non-hydrogen atoms were refined anisotropically except for the methyl carbon atoms of one rotationally disordered *t*Bu group. A split atom model was applied. The site occupancies of the respective orientations were refined as 0.74(1) (for C25a, C26a, C27a) and 0.26(1) (for C25b, C26b, C27b). Hydrogen atoms were assigned to idealized position and given a thermal parameter 1.2 times (1.5 for CH_3 groups) that of the atoms to which they are attached. No hydrogen atoms were calculated for the H_2O molecule. Final residuals: $R1$ = 0.0455, $wR2$ = 0.0855 (for 4593 reflections with $I > 2\sigma(I)$), $R1$ = 0.1342, $wR2$ = 0.1107 (for all data); 458 parameters; largest difference peak/hole: 0.575/ − 0.639 eÅ^{-3}.

Crystal data for $\mathbf{5}\cdot 2MeCN\cdot MeOH$: $C_{115}H_{142}B_2N_{20}Ni_4OS_4$ (M_r = 2205.18); crystal size 0.32 × 0.21 × 0.20 mm^3; monoclinic, space group $P2_1/n$ (no. 14), with a = 17.695(4), b = 17.647(4), c = 18.081(4) Å, β = 101.03(3)°, Z = 2 (the asymmetric unit of $\mathbf{5}\cdot 2MeCN\cdot MeOH$ consists of one half of the formula unit), V = 5542(2) Å^3, ρ_{calcd} = 1.322 g cm^{-3}, $2\theta_{max}$ = 56.78°, $\mu(Mo_{K\alpha})$ = 0.803 mm^{-1}, 49056 reflections measured, 13171 unique (R_{int} = 0.0785), 7379 observed reflections [$I > 2\sigma(I)$]; solution and refinement as for **4**. All non-hydrogen atoms were refined anisotropically except for the methyl carbon atoms of one rotationally disordered *t*Bu group. A split atom model was applied. The site occupancies of the respective orientations were refined as 0.57(1) (for C10a, C11a, C12a) and 0.43(1) (for C10b, C11b, C12b). The acetonitrile molecule is also disordered over two positions (0.50, 0.50). Hydrogen atoms were assigned to idealized position and given a thermal parameter 1.2 times (1.5 for CH_3 groups) that of the atoms to which they are attached. No hydrogen atoms were calculated for the CH_3CN molecule. Final residuals: $R1$ = 0.0576, $wR2$ = 0.1520 (for 7379 reflections with $I > 2\sigma(I)$), $R1$ = 0.1137, $wR2$ = 0.1813 (for all data); 648 parameter 648; largest difference peak/hole 0.880/ − 0.414 eÅ^{-3}. Crystallographic data (excluding structure factors) for the structures reported in this paper have been deposited with the Cambridge Crystallographic Data Centre as supplementary publication nos. CCDC-161832 (**4**) and CCDC-161833 (**5**). Copies of the data can be obtained free of charge on application to CCDC, 12 Union Road, Cambridge CB2 1EZ, UK (fax: (+44) 1223 336-033; e-mail: deposit@ccdc.cam.ac.uk).

Acknowledgements

We thank Prof. Dr. K. Wieghardt for providing facilities for susceptibility measurements. Drs. E. Bill and J. J. Girerd are thanked for giving lectures on magnetic exchange interactions in polynuclear complexes in Freiburg. Financial support of this work from the Deutsche Forschungsgemeinschaft (Graduiertenkolleg Ungepaarte Elektronen) is gratefully acknowledged. We also thank Prof. Dr. H. Vahrenkamp for his generous support.

[1] a) R. Sessoli, H.-L. Tsai, A. R. Schake, S. Wang, J. B. Vincent, K. Folting, D. Gatteschi, G. Christou, D. N. Hendrickson, *J. Am. Chem. Soc.* **1993**, *115*, 1804–1816; b) R. Sessoli, D. Gatteschi, A. Caneschi, M. A. Novak, *Nature* **1993**, *365*, 141–143; c) H. J. Eppley, H.-L. Tsai, N. de Vries, K. Folting, G. Christou, D. N. Hendrickson, *J. Am. Chem. Soc.* **1995**, *117*, 301–317; d) L. Thomas, F. Lionti, R. Ballou, D. Gatteschi, R. Sessoli, B. Barbara, *Nature* **1996**, *383*, 145–147; e) D. Ruiz, Z. Sun, B. Albela, K. Folting, J. Ribas, G. Christou, D. N. Hendrickson, *Angew. Chem.* **1998**, *110*, 315–318; *Angew. Chem. Int. Ed.* **1998**, *37*, 300–302; f) C. J. Matthews, K. Avery, Z. Xu, L. K. Thompson, L. Zhao, D. O. Miller, K. Biradha, K. Poirier, M. J. Zaworotko, C. Wilson, A. E. Goeta, J. A. K. Howard, *Inorg. Chem.* **1999**, *38*, 5266–5276; g) D. Gatteschi, R. Sessoli, A. Cornia, *Chem. Commun.* **2000**, 725–732; h) C. Benelli, A. J. Blake, E. K. Brechin, S. J. Coles, A. Graham, S. G. Harris, S. Meier, A. Parkin, S. Parsons, A. M. Seddon, R. E. P. Winpenny, *Chem. Eur. J.* **2000**, *6*, 883–-896; i) J. Larionova, M. Gross, M. Pilkington, H. Andres, H. Stoeckli-Evans, H. U. Güdel, S. Decurtins, *Angew. Chem.* **2000**, *112*, 1667–1672; *Angew. Chem. Int. Ed.* **2000**, *39*, 1605–1609.

[2] a) J. M. Lehn, *Supramolecular Chemistry: Concepts and Perspectives*, VCH, Weinheim, **1995**; b) R. W. Saalfrank, B. Demleitner in *Perspectives in Supramolecular Chemistry*, *Vol. 5* (Ed. J. P. Sauvage), Wiley-VCH, Weinheim, **1999**, pp. 1–51.

[3] a) C. S. Campos-Fernandez, R. Clerac, K. R. Dunbar, *Angew. Chem.* **1999**, *111*, 3685–3688; *Angew. Chem. Int. Ed.* **1999**, *38*, 3477–3479; b) L. Zhao, Z. Xu, L. K. Thompson, S. L. Heath, D. O. Miller, M. Ohba, *Angew. Chem.* **2000**, *112*, 3244–3247; *Angew. Chem. Int. Ed.* **2000**, *39*, 3114–3117; c) R. W. Saalfrank, S. Trummer, U. Reimann, M. M. Chowdhry, F. Hampel, O. Waldmann, *Angew. Chem.* **2000**, *112*, 3634–3636; *Angew. Chem. Int. Ed.* **2000**, *39*, 3492–3494 d) L. Zhao,

C. J. Matthews, L. K. Thompson, S. L. Heath, *Chem. Commun.* **2000**, 265 – 266.
[4] a) B. Kersting, D. Siebert, *Inorg. Chem.* **1998**, *37*, 3820 – 3828; b) B. Kersting, D. Siebert, D. Volkmer, M. J. Kolm, C. Janiak, *Inorg. Chem.* **1999**, *38*, 3871 – 3882.
[5] B. Kersting, G. Steinfeld, J. Hausmann, *Eur. J. Inorg. Chem.* **1999**, 179 – 187.
[6] F. A. Cotton, G. Wilkinson, *Advanced Inorganic Chemistry*, *6th ed.*, Wiley, New York, **1999**.
[7] The maximum value of $\chi_M T$ is about as large as the spin-only value of 3.34 $cm^3 Kmol^{-1}$ (5.17 μ_B) for $S_T = 2$ resulting from the ferromagnetic coupling of two Ni^{II} ions ($S_1 = S_2 = 1$, $g = 2.11$).
[8] Compounds **4** and **5** are both EPR-active. The X-band EPR spectra of powdered samples recorded at 4 K are consistent with an $S_T = 2$ for **4** and an $S_T = 4$ for **5** (E. Bill, private communication).
[9] The abrupt decrease in $\chi_M T$ below 5 K is presumably due to zero-field splitting of Ni^{II} or to saturation effects.
[10] S. Mohanta, K. K. Nanda, R. Werner, W. Haase, A. K. Mukherjee, S. K. Dutta, K. Nag, *Inorg. Chem.* **1997**, *36*, 4656 – 4664.
[11] a) J. B. Goodenough, *Phys. Rev.* **1955**, *100*, 564 – 573; b) J. Kanamori, *J. Phys. Chem. Solids*, **1959**, *10*, 87 – 98; c) A. P. Ginsberg, *Inorg. Chim. Acta Rev.* **1971**, *5*, 45 – 68.
[12] a) T. Beissel, F. Birkelbach, E. Bill, T. Glaser, F. Kesting, C. Krebs, T. Weyhermüller, K. Wieghardt, C. Butzlaff, A. X. Trautwein, *J. Am. Chem. Soc.* **1996**, *118*, 12376 – 12390; b) U. Bossek, D. Nühlen, E. Bill, T. Glaser, C. Krebs, T. Weyhermüller, K. Wieghardt, M. Lengen, A. X. Trautwein, *Inorg. Chem.* **1997**, *36*, 2834 – 2843.
[13] a) A. P. Ginsberg, R. L. Martin, R. C. Sherwood, *Inorg. Chem.* **1968**, *7*, 932 – 936; b) G. J. Bullen, R. Mason, P. Pauling, *Inorg. Chem.* **1965**, *4*, 456 – 462.
[14] Y. Elerman, M. Kabak, I. Svoboda, H. Fuess, K. Griesar, W. Haase, *Z. Naturforsch. B* **1996**, *51*, 1132 – 1136.
[15] a) A. Escuer, R. Vicente, J. Ribas, M. S. El Fallah, X. Solans, M. Font-Bardia, *Inorg. Chem.* **1993**, *32*, 3727 – 3732; b) A. Escuer, R. Vicente, M. S. El Fallah, J. Ribas, X. Solans, M. Font-Bardía, *J. Chem. Soc. Dalton Trans.* **1993**, 2975 – 2976; c) A. Escuer, R. Vicente, J. Ribas, M. S. El Fallah, X. Solans, M. Font-Bardía, *Inorg. Chem.* **1994**, *33*, 1842 – 1847; d) R. Vicente, A. Escuer, J. Ribas, M. S. El Fallah, X. Solans, M. Font-Bardía, *Inorg. Chem.* **1995**, *34*, 1278 – 1281; e) J. Ribas, M. Montfort, B. K. Ghosh, R. Cortés, X. Solans, M. Font-Bardía, *Inorg. Chem.* **1996**, *35*, 864 – 868.
[16] a) A. Escuer, C. J. Harding, Y. Dussart, J. Nelson, V. McKee, R. Vicente, *J. Chem. Soc. Dalton Trans.* **1999**, 223 – 227; b) C. S. Hong, Y. Do, *Angew. Chem.* **1999**, *111*, 153 – 155; *Angew. Chem. Int. Ed.* **1999**, *38*, 193 – 195; c) M. Montfort, I. Resino, J. Ribas, H. Stoeckli-Evans, *Angew. Chem.* **2000**, *112*, 197 – 199; *Angew. Chem. Int. Ed.* **2000**, *39*, 191 – 193.
[17] a) J. A. Bertrand, A. P. Ginsberg, R. I. Kaplan, C. E. Kirkwood, R. L. Martin, R. C. Sherwood, *Inorg. Chem.* **1971**, *10*, 240 – 246; b) W. L. Gladfelter, M. W. Lynch, W. P. Schaefer, D. N. Hendrickson, H. B. Gray, *Inorg. Chem.* **1981**, *20*, 2390 – 2397; c) L. Ballester, E. Coronado, A. Gutiérrez, A. Monge, M. F. Perpiñan, E. Pinilla, T. Rico, *Inorg. Chem.* **1992**, *32*, 2053 – 2056; d) J. Ribas, M. Monfort, R. Costa, X. Solans, *Inorg. Chem.* **1993**, *32*, 695 – 699; e) M. A. Halcrow, J. C. Huffman, G. Christou, *Angew. Chem.* **1995**, *107*, 971 – 973; *Angew. Chem. Int. Ed. Engl.* **1995**, *34*, 889 – 891; f) Z. E. Serna, L. Lezama, M. K. Urtiaga, M. I. Arriortua, M. G. Barandika, R. Cortes, T. Rojo, *Angew. Chem.* **2000**, *112*, 352 – 355; *Angew. Chem. Int. Ed.* **2000**, *39*, 344 – 347.
[18] SAINT, Version 4.050, Siemens Analytical X-ray Instruments Inc., Madison, WI, **1995**.
[19] G. M. Sheldrick, SADABS, University of Göttingen, **1997**.
[20] G. M. Sheldrick, *Acta Crystallogr. Sect. A* **1990**, *46*, 467 – 473.
[21] G. M. Sheldrick, SHELXL-93, a program for crystal structure refinement, University of Göttingen, **1993**.

Received: April 12, 2001 [F3195]

  0947-6539/01/0719-4258 $ 17.50+.50/0